Bit Error Probability for Pilot-Symbol-Aided OFDM Channel Estimation in Doubly-Selective Channels

Ronald Nissel, Martin Lerch, Michal Šimko and Markus Rupp
Institute of Telecommunications, Vienna University of Technology, Vienna, Austria
Email: {rnissel, mlerch, msimko, mrupp}@nt.tuwien.ac.at

***Abstract*—In this paper, we derive a closed-form expression for the Bit Error Probability (BEP) of an orthogonal frequency-division multiplexing system that utilizes pilot-symbol-aided channel estimation. We assume Rayleigh fading, additive white Gaussian noise, and that the interpolation is linear but otherwise completely arbitrary. It is shown that the minimum mean squared error interpolation also minimizes the BEP. For a Signal-to-Interference Ratio (SIR) smaller than the signal-to-noise ratio, simulations confirm our analytical results. However, for higher SIR they exhibit differences because the inter-carrier interference is not normally distributed, violating our assumptions.**

I. Introduction

Nowadays, most wireless communication standards (DAB, LTE, WIFI 802.11) utilize Orthogonal Frequency Division Multiplexing (OFDM) as their modulation technique. For coherent detection, the performance of such systems depends strongly on the accuracy of the channel estimation whereas one possible estimation technique is based on pilot-symbols. Here, in a first step, the channel at pilot positions is estimated by known symbols. In a second step, the channel at data positions is estimated by interpolation. Although the Mean Squared Error (MSE) allows for a comparison of different interpolation methods [1], [2], the Bit Error Probability (BEP) is a more intuitive measure. Authors of [3]–[5] compared different interpolation methods (e.g., "linear"[1], spline, low-pass) in terms of Bit Error Ratio (BER). However, their comparison is only based on simulations, not offering analytical insight. We therefore derive a closed-form solution of the BEP under channel estimation for arbitrary linear interpolation methods. We restrict ourselves to the case of 4-Quadrature Amplitude Modulation (QAM) and 16-QAM but the proposed method can straightforwardly be extended to higher modulation orders.

The transmitted data-symbols are corrupted by a doubly-selective channel, i.e., frequency-selective as well as time-selective, the latter causing Inter-Carrier Interference (ICI). Some authors model ICI as Gaussian noise, claiming that the central limit theorem can be applied. This approximation is false as shown in [6] which means that, depending on ICI, our calculated BEP that is based on the Gaussian assumption, may exhibit a deviation.

Our analysis can also be applied to subspace techniques such as Slepian basis expansion models [7], but does not include ICI mitigation [8] or iterative receivers [9].

[1] in the geometrical sense of a straight line

II. System Model

In our OFDM model, $x_{l,k} \in \mathbb{C}$ denotes the transmitted data symbol at subcarrier-position l ($l = 1, 2 \ldots, L$) and time-position k ($k = 0, 1 \ldots, K-1$) and is chosen from a 4-QAM respectively 16-QAM signal constellation. The received data symbols $\mathbf{y}_k = [\ y_{1,k} \quad \ldots \quad y_{L,k}\ ]^T \in \mathbb{C}^{L\times 1}$ depends on the transmitted data symbols $\mathbf{x}_k = [\ x_{1,k} \quad \ldots \quad x_{L,k}\ ]^T \in \mathbb{C}^{L\times 1}$ as follows:

$$\mathbf{y}_k = \mathbf{D}_k \mathbf{x}_k + \mathbf{z}_k, \tag{1}$$

where the noise vector $\mathbf{z}_k \in \mathbb{C}^{L\times 1}$ is assumed to be white complex Gaussian with zero mean $\mathbf{z}_k \sim \mathcal{CN}(0, \mathbf{R}_{\mathbf{z}_k})$. The l-th row and d-th column element of the OFDM matrix $\mathbf{D}_k \in \mathbb{C}^{L\times L}$ is given as:

$$(\mathbf{D}_k)_{l,d} = \frac{1}{N}\sum_{n=0}^{N-1} H[n + k(N+N_{\mathrm{cp}}), d]\mathrm{e}^{-\mathrm{j}2\pi\frac{l-d}{N}n}, \tag{2}$$

where $H[m, l] \in \mathbb{C}$ denotes the sampled time-variant transfer function[2], N the length of the OFDM symbol and N_{cp} the length of the cyclic prefix.

We consider the ICI part as an additional noise term (no ICI mitigation) so that Equation (1) can be reformulated as:

$$y_{l,k} = h_{l,k}x_{l,k} + y_{\mathrm{ICI}_{l,k}} + z_{l,k}, \tag{3}$$

where the channel $h_{l,k} \in \mathbb{C}$ can be found as the l-th diagonal element of the OFDM matrix $\mathbf{D}_k$. Dividing Equation (3) by the estimated channel $\hat{h}_{l,k}$ leads to the zero forcing (Least Squares (LS)) equalization and delivers an estimate of the transmitted data symbol $x_{l,k}$:

$$\hat{x}_{l,k} = \frac{y_{l,k}}{\hat{h}_{l,k}}. \tag{4}$$

Regarding statistical properties, we make the following assumptions:

- channel, noise, and data symbols are statistically independent from each other
- the mean channel power is normalized to one
- the data symbols are statistically independent, have zero mean, and are normalized to have mean power one.

[2] defined for the discrete-time samples $m = 0, 1, \ldots, K(N+N_{\mathrm{cp}}) - N_{\mathrm{cp}} - 1$ and the discrete-frequency samples $l = 1, 2 \ldots, L$

ISBN 978-3-8007-3584-6

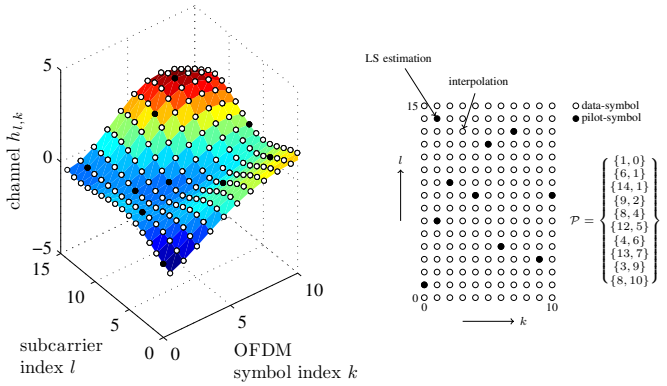

Fig. 1. Pilot-symbol-aided channel estimation utilizing an arbitrary pilot pattern.

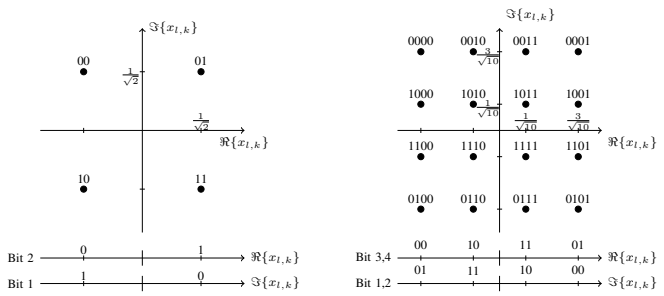

Fig. 2. 4-QAM (left) and 16-QAM (right) applying Gray code.

The received data symbol power $\mathbb{E}\{y_{l,k}y_{l,k}^*\}$ is then given as a summation of the signal power $P_{\mathrm{S}_{l,k}}$, the ICI power $P_{\mathrm{ICI}_{l,k}}$, and the noise power $P_{\mathrm{noise}_{l,k}} \in \mathbb{R}$:

$$\mathbb{E}\{y_{l,k}y_{l,k}^*\} = \underbrace{\mathbb{E}\left\{\left|(\mathbf{D}_k)_{l,l}\right|^2\right\}}_{P_{\mathrm{S}_{l,k}}} + \underbrace{\sum_{\substack{d=1\\d\neq l}}^{L}\mathbb{E}\left\{\left|(\mathbf{D}_k)_{l,d}\right|^2\right\}}_{P_{\mathrm{ICI}_{l,k}}} + \underbrace{\mathbb{E}\left\{|z_{l,k}|^2\right\}}_{P_{\mathrm{noise}_{l,k}}}. \quad (5)$$

III. Bit Error Probability for Pilot-Symbol-Aided Channel Estimation

The channel estimates at pilot positions are obtained by an LS-estimation which minimizes the error of the L^2 norm and requires no statistical knowledge:

$$\hat{h}_{l,k}^{\mathrm{LS}} = \arg\min_{\tilde{h}_{l,k}} \|y_{l,k} - \tilde{h}_{l,k}x_{l,k}\|_2^2 = \frac{y_{l,k}}{x_{l,k}}. \quad (6)$$

The channel estimations at data position can then be obtained by interpolation, i.e., a weighted average of the known LS estimations:

$$\hat{h}_{l,k} = \sum_{\{l_p,k_p\}\in\mathcal{P}} \left(\mathbf{w}_{l,k}^*\right)_{\{l_p,k_p\}} \frac{y_{l_p,k_p}}{x_{l_p,k_p}}. \quad (7)$$

The set $\mathcal{P}$ is a collection of the two-dimensional (2D) pilot position indexes, as illustrated in Figure 1. The number of pilot symbols is given by $|\mathcal{P}|$. Equation (7) can also be written in vector notation as:

$$\hat{h}_{l,k} = \mathbf{w}_{l,k}^H \hat{\mathbf{h}}_{\mathcal{P}}^{\mathrm{LS}}, \quad (8)$$

where the vector $\hat{\mathbf{h}}_{\mathcal{P}}^{\mathrm{LS}} \in \mathbb{C}^{|\mathcal{P}|\times 1}$ consists of the vectorized LS estimates at pilot positions. The weighting vector $\mathbf{w}_{l,k} \in \mathbb{C}^{|\mathcal{P}|\times 1}$ depends on the interpolation method (e.g., Minimum Mean Squared Error (MMSE), "linear", spline).

In order to compare different interpolation methods $\mathbf{w}_{l,k}$, we derive the BEP for arbitrary weighting vectors. We make the following assumptions regarding the pilot symbols:

- every pilot symbol has unit magnitude.
- the pilot symbols are random, statistically independent variables of zero mean.
- known pilot symbols have no significant effect on the statistic of the ICI.

The last assumption guarantees that the MMSE channel estimation is independent of concrete pilots symbols. Furthermore, we assume that channel coefficients and noise samples are Gaussian random variables.

The calculation of the BEP is based on [10], [11] where in particular we make use of the following lemma:

Lemma 1: Let X and Y be zero mean, correlated complex-valued Gaussian random variables, then

$$\Pr\left(\Re\{XY^*\} < 0\right) = \frac{1}{2}\left[1 - \frac{\Re\{\mathbb{E}\{XY^*\}\}}{\sqrt{\mathbb{E}\{XX^*\}\mathbb{E}\{YY^*\} - (\Im\{\mathbb{E}\{XY^*\}\})^2}}\right]. \quad (9)$$

Consider 4-QAM, then the probability that the second bit is wrongfully detected as a "0", while a "1" was sent (see Figure 2), is given by the law of total probability as the average of $\Pr\left(\Re\{\hat{x}_{l,k}\} < 0 \middle| \frac{1+\mathrm{j}}{\sqrt{2}}\right)$ and $\Pr\left(\Re\{\hat{x}_{l,k}\} < 0 \middle| \frac{1-\mathrm{j}}{\sqrt{2}}\right)$. Because of symmetry, this probability represents also the case for all other bit errors (they can be rotated to the above described case), so that the BEP can be written as:

$$\begin{aligned}\mathrm{BEP}_{l,k}^{4\mathrm{QAM}}(\mathbf{w}_{l,k}) =& \frac{1}{2}\Pr\left(\Re\left\{\frac{y_{l,k}}{\hat{h}_{l,k}}\right\} < 0 \middle| \frac{1+\mathrm{j}}{\sqrt{2}}\right) \\ &+ \frac{1}{2}\Pr\left(\Re\left\{\frac{y_{l,k}}{\hat{h}_{l,k}}\right\} < 0 \middle| \frac{1-\mathrm{j}}{\sqrt{2}}\right).\end{aligned} \quad (10)$$

In a similar way, the BEP of the second and fourth bit for 16-QAM, can be found as:

$$\mathrm{BEP}_{l,k}^{16\mathrm{QAM,Bit2\&4}}(\mathbf{w}_{l,k}) = \frac{1}{8}\sum_{\substack{q_r\in\\\{1,3\}}}\sum_{\substack{q_i\in\{-3,\\-1,1,3\}}}\Pr\left(\Re\left\{\frac{y_{l,k}}{\hat{h}_{l,k}}\right\} < 0 \middle| \frac{q_r+\mathrm{j}q_i}{\sqrt{10}}\right), \quad (11)$$

ISBN 978-3-8007-3584-6

$$\Pr\left(\Re\left\{\frac{y_{l,k}}{\hat{h}_{l,k}}\right\} < \frac{a}{\sqrt{b}}\middle|\frac{q_r+\mathrm{j}q_i}{\sqrt{b}}\right) = \frac{1}{2} - \frac{1}{2}\Big[q_r\Re\{\alpha_{l,k}\} - q_i\Im\{\alpha_{l,k}\} - a\beta_{l,k}\Big]\times \\ \times\left[\big[(q_r^2+q_i^2)P_{\mathrm{S}_{l,k}} + bP_{\mathrm{noise}_{l,k}} - 2a\left(q_r\Re\{\alpha_{l,k}\} - q_i\Im\{\alpha_{l,k}\}\right) + a^2\beta_{l,k}\big]\beta_{l,k} - \left(q_i\Re\{\alpha_{l,k}\} + q_r\Im\{\alpha_{l,k}\}\right)^2\right]^{-\frac{1}{2}} \tag{12}$$

and for the first and third bit:

$$\mathrm{BEP}_{l,k}^{16\mathrm{QAM,Bit1\&3}}(\mathbf{w}_{l,k}) = \\ \frac{1}{8}\sum_{\substack{q_i\in\{-3,\\-1,1,3\}}}\left(1-\Pr\left(\frac{-2}{\sqrt{10}} < \Re\left\{\frac{y_{l,k}}{\hat{h}_{l,k}}\right\} < \frac{2}{\sqrt{10}}\middle|\frac{1+\mathrm{j}q_i}{\sqrt{10}}\right)\right) \\ + \frac{1}{8}\sum_{\substack{q_i\in\{-3,\\-1,1,3\}}}\Pr\left(\frac{-2}{\sqrt{10}} < \Re\left\{\frac{y_{l,k}}{\hat{h}_{l,k}}\right\} < \frac{2}{\sqrt{10}}\middle|\frac{3+\mathrm{j}q_i}{\sqrt{10}}\right). \tag{13}$$

The overall BEP for 16-QAM is then simply the average of Equation (11) and (13).

$$\mathrm{BEP}_{l,k}^{16\mathrm{QAM}}(\mathbf{w}_{l,k}) = \\ \frac{1}{2}\mathrm{BEP}_{l,k}^{16\mathrm{QAM,Bit1\&3}}(\mathbf{w}_{l,k}) + \frac{1}{2}\mathrm{BEP}_{l,k}^{16\mathrm{QAM,Bit2\&4}}(\mathbf{w}_{l,k}). \tag{14}$$

In order to apply Lemma 1, the probabilities have to be rewritten as:

$$\begin{aligned}\Pr\left(\Re\left\{\frac{y_{l,k}}{\hat{h}_{l,k}}\right\} < a\middle|x_{l,k}\right) &= \\ &= \Pr\left(\Re\left\{y_{l,k}\hat{h}_{l,k}^*\right\} < a\hat{h}_{l,k}\hat{h}_{l,k}^*\middle|x_{l,k}\right) \\ &= \Pr\left(\Re\left\{\left(y_{l,k}-a\hat{h}_{l,k}\right)\hat{h}_{l,k}^*\right\} < 0\middle|x_{l,k}\right).\end{aligned} \tag{15}$$

Because the received symbol $y_{l,k}$ as well as the channel estimate $\hat{h}_{l,k}$ are Gaussian variables (conditioned on the transmitted data symbol $x_{l,k}$), Lemma 1 can be applied. The required cross- and auto correlations at data position are given as:

$$\mathbb{E}\left\{\left(y_{l,k}-a\hat{h}_{l,k}\right)\hat{h}_{l,k}^*\middle|x_{l,k}\right\} = \\ \mathbf{r}_{\hat{\mathbf{h}}_{\mathcal{P}}^{\mathrm{LS}},h_{l,k}}^H\mathbf{w}_{l,k}x_{l,k} - a\mathbf{w}_{l,k}^H\mathbf{R}_{\hat{\mathbf{h}}_{\mathcal{P}}^{\mathrm{LS}}}\mathbf{w}_{l,k} \tag{16}$$

$$\mathbb{E}\left\{\left|y_{l,k}-a\hat{h}_{l,k}\right|^2\middle|x_{l,k}\right\} = P_{\mathrm{S}_{l,k}}x_{l,k}x_{l,k}^* + P_{\mathrm{ICI}_{l,k}} + P_{\mathrm{noise}_{l,k}} \\ - 2a\Re\left\{\mathbf{r}_{\hat{\mathbf{h}}_{\mathcal{P}}^{\mathrm{LS}},h_{l,k}}^H\mathbf{w}_{l,k}x_{l,k}\right\} + a^2\mathbf{w}_{l,k}^H\mathbf{R}_{\hat{\mathbf{h}}_{\mathcal{P}}^{\mathrm{LS}}}\mathbf{w}_{l,k} \tag{17}$$

$$\mathbb{E}\left\{\hat{h}_{l,k}\hat{h}_{l,k}^*\right\} = \mathbf{w}_{l,k}^H\mathbf{R}_{\hat{\mathbf{h}}_{\mathcal{P}}^{\mathrm{LS}}}\mathbf{w}_{l,k}. \tag{18}$$

The cross-correlation vector $\mathbf{r}_{\hat{\mathbf{h}}_{\mathcal{P}}^{\mathrm{LS}},h_{l,k}} = \mathbb{E}\{\hat{\mathbf{h}}_{\mathcal{P}}^{\mathrm{LS}}h_{l,k}^*\} \in \mathbb{C}^{|\mathcal{P}|\times 1}$ and the autocorrelation matrix $\mathbf{R}_{\hat{\mathbf{h}}_{\mathcal{P}}^{\mathrm{LS}}} = \mathbb{E}\{\hat{\mathbf{h}}_{\mathcal{P}}^{\mathrm{LS}}(\hat{\mathbf{h}}_{\mathcal{P}}^{\mathrm{LS}})^H\} \in \mathbb{C}^{|\mathcal{P}|\times|\mathcal{P}|}$ themselves can be obtained by:

$$\mathbf{R}_{\hat{\mathbf{h}}_{\mathcal{P}}^{\mathrm{LS}}} = \mathbf{R}_{\mathbf{h}_{\mathcal{P}}} + \mathrm{diag}\left(\mathbf{p}_{\mathrm{ICI}_{\mathcal{P}}} + \mathbf{p}_{\mathrm{noise}_{\mathcal{P}}}\right) \tag{19}$$

$$\mathbf{r}_{\hat{\mathbf{h}}_{\mathcal{P}}^{\mathrm{LS}},h_{l,k}} = \mathbf{r}_{\mathbf{h}_{\mathcal{P}},h_{l,k}}. \tag{20}$$

The vectors $\mathbf{p}_{\mathrm{ICI}_{\mathcal{P}}}, \mathbf{p}_{\mathrm{noise}_{\mathcal{P}}} \in \mathbb{R}^{|\mathcal{P}|\times 1}$ consists of the vectorized ICI- respectively noise-powers at pilot position (Equation (5)) and the $\mathrm{diag}(\cdot)$ operator creates a diagonal matrix out of a vector.

By applying Lemma 1 and inserting Equation (16)-(18) in Equation (15), a general expression for the probability can be found. For a compact description we define two new variables, $\alpha_{l,k} \in \mathbb{C}$ and $\beta_{l,k} \in \mathbb{R}$:

$$\alpha_{l,k} = \mathbf{r}_{\hat{\mathbf{h}}_{\mathcal{P}}^{\mathrm{LS}},h_{l,k}}^H\mathbf{w}_{l,k} \tag{21}$$

$$\beta_{l,k} = \mathbf{w}_{l,k}^H\mathbf{R}_{\hat{\mathbf{h}}_{\mathcal{P}}^{\mathrm{LS}}}\mathbf{w}_{l,k}, \tag{22}$$

so that the probability can be expressed by Equation (12), which can be applied in Equation (10), (11), and (13) to find a closed form solution for the BEP.

For the special case[3] of $\Im\{\mathbf{r}_{\hat{\mathbf{h}}_{\mathcal{P}}^{\mathrm{LS}},h_{l,k}}^H\mathbf{w}_{l,k}\} = 0$ (interpolation compensates average phase shifts) and $\Re\{\mathbf{r}_{\hat{\mathbf{h}}_{\mathcal{P}}^{\mathrm{LS}},h_{l,k}}^H\mathbf{w}_{l,k}\} > 0$ (interpolation is better than a random guess), the BEP for 4-QAM can be written as:

$$\widetilde{\mathrm{BEP}}_{l,k}^{4\mathrm{QAM}}(\mathbf{w}_{l,k}) = \\ \frac{1}{2} - \frac{1}{2\sqrt{2(P_{\mathrm{S}_{l,k}}+P_{\mathrm{ICI}_{l,k}}+P_{\mathrm{noise}_{l,k}})\frac{\mathbf{w}_{l,k}^H\mathbf{R}_{\hat{\mathbf{h}}_{\mathcal{P}}^{\mathrm{LS}}}\mathbf{w}_{l,k}}{\left(\mathbf{r}_{\hat{\mathbf{h}}_{\mathcal{P}}^{\mathrm{LS}},h_{l,k}}^H\mathbf{w}_{l,k}\right)^2}-1}}. \tag{23}$$

In order to minimize Equation (23), the generalized Rayleigh quotient inside the square root has to be minimized, or equivalently, the inverse quotient $\frac{\mathbf{w}_{l,k}^H\mathbf{r}_{\hat{\mathbf{h}}_{\mathcal{P}}^{\mathrm{LS}},h_{l,k}}\mathbf{r}_{\hat{\mathbf{h}}_{\mathcal{P}}^{\mathrm{LS}},h_{l,k}}^H\mathbf{w}_{l,k}}{\mathbf{w}_{l,k}^H\mathbf{R}_{\hat{\mathbf{h}}_{\mathcal{P}}^{\mathrm{LS}}}\mathbf{w}_{l,k}}$ maximized. Since the matrices in the nominator and denominator are Hermitian, this maximization becomes a generalized eigenvalue problem

$$\mathbf{r}_{\hat{\mathbf{h}}_{\mathcal{P}}^{\mathrm{LS}},h_{l,k}}\mathbf{r}_{\hat{\mathbf{h}}_{\mathcal{P}}^{\mathrm{LS}},h_{l,k}}^H\mathbf{w}_{l,k} = \lambda\,\mathbf{R}_{\hat{\mathbf{h}}_{\mathcal{P}}^{\mathrm{LS}}}\mathbf{w}_{l,k}. \tag{24}$$

The unique solution for Equation (24) can be found by inserting the MMSE estimation [12]. The optimal interpolation for 4-QAM can thus be written as:

$$\begin{aligned}\mathbf{w}_{l,k}^{4\mathrm{QAM,minBEP}} &= \arg\min_{\mathbf{w}_{l,k}}\mathrm{BEP}_{l,k}^{4\mathrm{QAM}}(\mathbf{w}_{l,k}) \\ &= \mathbf{R}_{\hat{\mathbf{h}}_{\mathcal{P}}^{\mathrm{LS}}}^{-1}\mathbf{r}_{\hat{\mathbf{h}}_{\mathcal{P}}^{\mathrm{LS}},h_{l,k}} \\ &= \mathbf{w}_{l,k}^{\mathrm{MMSE}}.\end{aligned} \tag{25}$$

[3] the proposed method is not restricted to this special case. However, due to the length of the equations we omit the closed-form expression for the general case.

ISBN 978-3-8007-3584-6

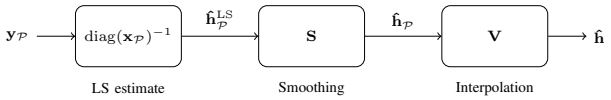

Fig. 3. Separated smoothing and interpolation [13].

Following along the same lines, the optimal interpolation for 16-QAM can be found as:

$$\begin{aligned}(\mathbf{w}_{l,k})^{16\mathrm{QAM,minBEP}} &= \arg\min_{\mathbf{w}_{l,k}} \mathrm{BEP}_{l,k}^{16\mathrm{QAM}}(\mathbf{w}_{l,k}) \\ &= \kappa_{l,k}\mathbf{R}^{-1}_{\hat{\mathbf{h}}_\mathcal{P}^{\mathrm{LS}}}\mathbf{r}_{\hat{\mathbf{h}}_\mathcal{P}^{\mathrm{LS}},h_{l,k}},\end{aligned} \tag{26}$$

whereas for low signal-to-noise ratios the real valued scaling factor $\kappa_{l,k}$ is larger then one and for large ratios it has to be smaller. However, numerical evaluations have shown that Equation (26) improves the $\mathrm{BEP}_{l,k}^{16\mathrm{QAM}}$ only by less than 1% so that the differences between $\mathbf{w}_{l,k}^{16\mathrm{QAM,minBEP}}$ and $\mathbf{w}_{l,k}^{\mathrm{MMSE}}$ can be neglected.

Equation (23) can also be used to calculate the BEP in case of perfect channel knowledge by inserting the MMSE interpolation and setting the MSE to zero, which leads to:

$$\mathrm{BEP}_{l,k}^{4\mathrm{QAM,perfect}} = \frac{1}{2} - \frac{1}{2\sqrt{1+2\frac{P_{\mathrm{ICI}_{l,k}}+P_{\mathrm{noise}_{l,k}}}{P_{\mathrm{S}_{l,k}}}}}. \tag{27}$$

The same approach can be straightforwardly extended to find a solution for 16-QAM under perfect channel knowledge.

IV. Interpolation

As explained in Section III, the channel estimation $\hat{h}_{l,k}$ can be obtained as:

$$\hat{h}_{l,k} = \mathbf{w}_{l,k}^H \hat{\mathbf{h}}_\mathcal{P}^{\mathrm{LS}}, \tag{28}$$

where $\mathbf{w}_{l,k}$ represents the interpolation vector. Because such an estimation is linear, the weighting vector can be separated in a smoothing and an interpolation part (see Figure 3), as suggested in [13]. The smoothing part reduces noise at pilot positions while the interpolation part can be designed to be independent of noise. Such a separation provides the opportunity to identify whether some improvements are caused by interpolation or by more accurate estimations at pilot positions. The vectorized channel estimation $\hat{\mathbf{h}} \in \mathbb{C}^{LK\times 1}$ can then be written as

$$\hat{\mathbf{h}} = \mathbf{V}\mathbf{S}\hat{\mathbf{h}}_\mathcal{P}^{\mathrm{LS}}, \tag{29}$$

whereby $\mathbf{S} \in \mathbb{C}^{|\mathcal{P}|\times|\mathcal{P}|}$ describes a smoothing and $\mathbf{V} \in \mathbb{C}^{LK\times|\mathcal{P}|}$ an interpolation matrix. Linearity also simplifies finding the matrix $\mathbf{V}$ because it can be interpreted as a shift-variant "impulse response": The i-th column vector of the matrix $\mathbf{V}$ can be found by applying the interpolation method to a vector that consist mainly of zeros except the i-th position, which is a one.

The optimal interpolation was also derived in Section III were it was found that the MMSE channel estimation also minimizes the BEP. The optimal smoothing and interpolation matrices can thus be written as:

$$\mathbf{V}^{\mathrm{LMMSE}} = \mathbf{R}_{\mathbf{h},\mathbf{h}_\mathcal{P}}\mathbf{R}_{\mathbf{h}_\mathcal{P}}^{-1} \tag{30}$$

$$\mathbf{S}^{\mathrm{LMMSE}} = \mathbf{R}_{\mathbf{h}_\mathcal{P}}\left(\mathbf{R}_{\mathbf{h}_\mathcal{P}} + \mathrm{diag}\left(\mathbf{p}_{\mathrm{ICI}_\mathcal{P}} + \mathbf{p}_{\mathrm{noise}_\mathcal{P}}\right)\right)^{-1}. \tag{31}$$

Note that, for a Wide-Sense Stationary Uncorrelated Scattering (WSSUS) channel, a rectangular-shaped pilot-symbol pattern, and a separable time-frequency correlation function, the optimal 2D interpolation $\mathbf{V}^{\mathrm{LMMSE}}$ can be performed in an equivalent way by successively applying two independent 1D interpolations, i.e., interpolation first in one direction, and then again in the other direction.

Whether some interpolation methods (e.g., "linear", spline) are optimal depends only on the correlation matrices. Even "linear" interpolation can be optimal. For that, as a necessary condition, the correlation function must exhibit a triangular shape.

V. Simulation

For the numerical simulation, we utilize the following sampled WSSUS channel model [14]:

$$H[m,l] = \lim_{I\to\infty}\frac{1}{\sqrt{I}}\sum_{i=1}^{I}\mathrm{e}^{\mathrm{j}\left(\theta_i+2\pi\nu_i\frac{T_s}{N}m-2\pi\tau_i\Delta f\, l\right)}, \tag{32}$$

which delivers a sampled time-variant transfer function $H[m,l]$ as used in Equation (2). The variable T_s denotes the length of the OFDM symbol in the time domain while Δf is the subcarrier spacing. Because of orthogonality, the following relationship holds: $T_s = 1/\Delta f$. The uniform distributed random phase θ_i ensures circularly symmetry. Note that $H[n,l]$ is described by a complex Gaussian process due to the central limit theorem. We further assume that the delays τ_i and the Doppler shifts ν_i are statistically independent from each other and it has got a uniform power delay profile respectively a Jakes Doppler spectral density, so that the time-frequency correlation function becomes [15]:

$$\mathbb{E}\left\{H[n_1,l_1]H^*[n_2,l_2]\right\} = r_{H_t}[n_1-n_2]r_{H_f}[l_1-l_2]. \tag{33}$$

with

$$r_{H_t}[n_1-n_2] = \mathrm{J}_0\left(2\pi\nu_{\max}T_s\frac{n_1-n_2}{N}\right) \tag{34}$$

$$r_{H_f}[l_1-l_2] = \mathrm{sinc}(\pi\tau_{\max}\Delta f(l_2-l_2)). \tag{35}$$

where J_0 is the zeroth-order Bessel function. Equation (35) describes the frequency correlation of the channel $h_{l,k}$, while the temporal-correlation has to be calculated as follows:

$$r_{\bar{H}_t}[k_1-k_2] = \frac{1}{N^2}\sum_{n_1=0}^{N-1}\sum_{n_2=0}^{N-1} r_{H_t}[n_1-n_2+(k_1-k_2)(N+N_{\mathrm{cp}})]. \tag{36}$$

The correlation matrix of the vectorized channel $\mathbf{h} \in \mathbb{C}^{LK\times 1}$ is then given as:

$$\begin{aligned}\mathbf{R}_\mathbf{h} = &\begin{bmatrix} r_{\bar{H}_t}[0] & \cdots & r_{\bar{H}_t}[-(K-1)] \\ \vdots & \ddots & \vdots \\ r_{\bar{H}_t}[(K-1)] & \cdots & r_{\bar{H}_t}[0] \end{bmatrix} \\ &\otimes \begin{bmatrix} r_{H_f}[0] & \cdots & r_{H_f}[-(L-1)] \\ \vdots & \ddots & \vdots \\ r_{H_f}[(L-1)] & \cdots & r_{H_f}[0] \end{bmatrix}.\end{aligned} \tag{37}$$

The correlation matrices $\mathbf{R}_{\mathbf{h},\mathbf{h}_\mathcal{P}} \in \mathbb{C}^{LK\times|\mathcal{P}|}$ and $\mathbf{R}_{\mathbf{h}_\mathcal{P}} \in \mathbb{C}^{|\mathcal{P}|\times|\mathcal{P}|}$ can then be obtained as the proper elements (determined by the vectorized pilot-indexes) of $\mathbf{R}_\mathbf{h}$. Finally, by

ISBN 978-3-8007-3584-6

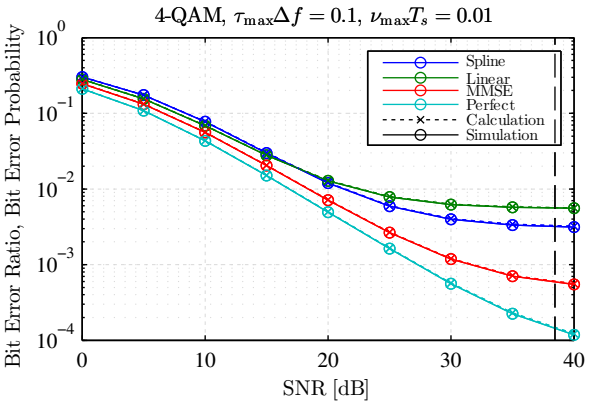

(a) BER vs. BEP as a function of SNR, influence of interpolation, simulation and calculation coincide.

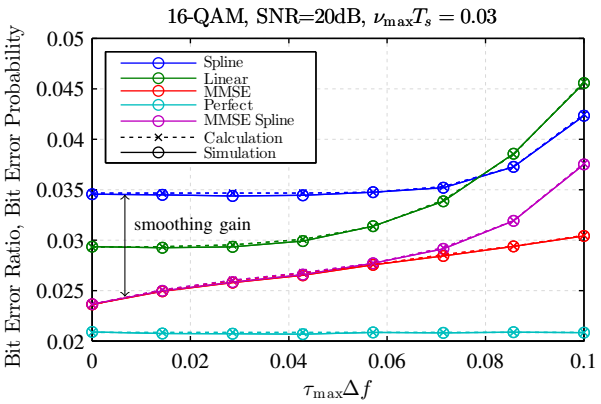

(b) BER vs. BEP as a function of the maximum normalized delay $\tau_{\max}\Delta f$, influence of interpolation, simulation and calculation coincide, spline interpolation in combination with MMSE smoothing performs well.

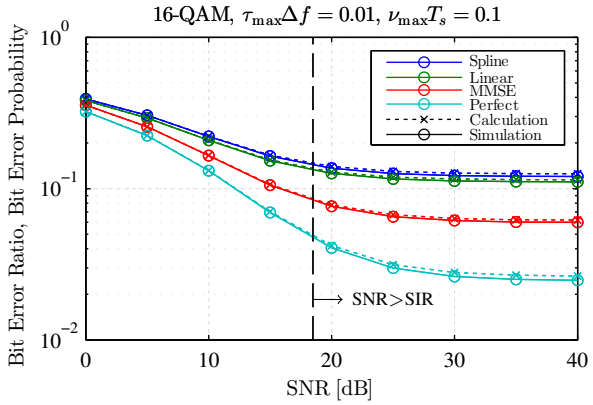

(c) BER vs. BEP as a function of SNR, influence of interpolation, simulations and calculations coincide for SNR<SIR. For higher SNR, they exhibit differences due to non-Gaussian ICI.

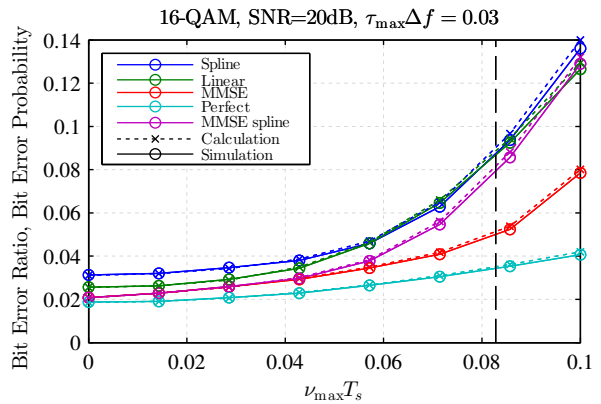

(d) BER vs. BEP as a function of the maximum normalized Doppler shift $\nu_{\max}T_s$, influence of interpolation, simulations and calculations coincide for SNR<SIR. For higher SNR, they exhibit differences due to non-Gaussian ICI.

Fig. 4. Bit Error Ratio vs. Bit Error Probability.

inserting these correlation matrices in Equation (19) and (20), a numerical result of the BEP can be obtained.

Our simulation is performed by applying Equation (2) to a channel $H[m,l]$, generated according to Equation (32) with $I = 1500$. Note that the channel model is very general in the sense that the delays τ_i and Doppler shift ν_i can be continuous and are not restricted by a specific sampling frequency. The drawback of such a method is the high computational complexity. We therefore choose only a low number of subcarriers and OFDM symbols ($L = 19$, $K = 13$). Furthermore, we use a rectangular-shaped pilot-symbol pattern with a time-spacing of 4 and a frequency-spacing of 6.

For the comparison of the calculated BEP with the simulated BER, we consider three specific interpolation methods: the 2D MMSE estimation given by Equation (25), a "linear"- and a spline[4]-interpolation [16]. The latter two are obtained by 1D interpolation first in one direction, and then again in the other direction. Note that the interpolation matrices $\mathbf{V}^{\text{spline}}$ and $\mathbf{V}^{\text{linear}}$ can be found by applying the method described in Section IV ("impulse response").

[4]we utilize the MATLAB build-in function

Figure 4a shows that simulation and calculation coincides, whereas in Figure 4c, the curves perfectly coincide only for a Signal-to-Noise Ratio (SNR) smaller than the Signal-to-Interference Ratio (SIR) due to non-Gaussian ICI. However, the maximal error of the analytical solution at high SNR is relatively low (less than 3%).

Figure 4b and 4d also confirm the analytical BEP expression if the noise power is larger than the ICI power. Note also that the BEP for perfect channel knowledge, provided the cyclic prefix is selected large enough, is independent of $\tau_{\max}\Delta f$, while it depends on $\nu_{\max}T_s$ due to ICI. Furthermore, Figure 4b and 4d shows the performance of spline interpolation applied to MMSE smoothed pilots. Numerical evaluation suggest that spline interpolation outperforms "linear" interpolation for highly doubly-selective channels or in combination with MMSE smoothing.

ISBN 978-3-8007-3584-6

VI. Conclusion

We derived the BEP expression for pilot-symbol-aided channel estimation utilizing arbitrary linear interpolation methods. We restricted ourself to 4-QAM and 16-QAM, but the proposed technique can straightforwardly be extended to higher modulation orders. The closed-form expression allows for a comprehensive comparison of different interpolation methods and pilot-symbol patterns. Simulations confirmed our analytical results for SNR<SIR, while for larger SNR they exhibit differences due to non-Gaussian ICI, violating our assumptions.

For 4-QAM, the MMSE interpolation also minimizes the BEP, while for 16-QAM this is accomplished by a scaled MMSE interpolation. However, the potential improvement compared to the unscaled MMSE interpolation is so low, that the scaling factor can be neglected.

Acknowledgment

This work has been funded by the Christian Doppler Laboratory for Wireless Technologies for Sustainable Mobility, the A1 Telekom Austria AG, and the KATHREIN-Werke KG. The financial support by the Federal Ministry of Economy, Family and Youth and the National Foundation for Research, Technology and Development is gratefully acknowledged.

References

[1] M. Simko, P. Diniz, Q. Wang, and M. Rupp, "Adaptive pilot-symbol patterns for MIMO OFDM systems," *IEEE Transactions on Wireless Communications*, vol. 12, no. 9, pp. 4705–4715, 2013.

[2] M. Meidlinger, M. Simko, Q. Wang, and M. Rupp, "Channel estimators for LTE-A downlink fast fading channels," in *Proc. of 17th International ITG Workshop on Smart Antennas (WSA 2013)*, Stuttgart, Germany, March 2013.

[3] X. Dong, W.-S. Lu, and A. Soong, "Linear interpolation in pilot symbol assisted channel estimation for OFDM," *IEEE Transactions on Wireless Communications*, vol. 6, no. 5, pp. 1910–1920, 2007.

[4] M.-H. Hsieh and C.-H. Wei, "Channel estimation for OFDM systems based on comb-type pilot arrangement in frequency selective fading channels," *IEEE Transactions on Consumer Electronics*, vol. 44, no. 1, pp. 217–225, 1998.

[5] S. Coleri, M. Ergen, A. Puri, and A. Bahai, "Channel estimation techniques based on pilot arrangement in OFDM systems," *IEEE Trans. Broadcasting*, vol. 48, pp. 223–229, 2002.

[6] T. Wang, J. Proakis, E. Masry, and J. Zeidler, "Performance degradation of OFDM systems due to Doppler spreading," *IEEE Transactions on Wireless Communications*, vol. 5, no. 6, pp. 1422–1432, 2006.

[7] T. Zemen and C. Mecklenbrauker, "Time-variant channel estimation using discrete prolate spheroidal sequences," *IEEE Transactions on Signal Processing*, vol. 53, no. 9, pp. 3597–3607, Sept 2005.

[8] F. Pena-Campos, R. Carrasco-Alvarez, O. Longoria-Gandara, and R. Parra-Michel, "Estimation of fast time-varying channels in OFDM systems using two-dimensional prolate," *IEEE Transactions on Wireless Communications*, vol. 12, no. 2, pp. 898–907, February 2013.

[9] P. Hammarberg, F. Rusek, and O. Edfors, "Iterative receivers with channel estimation for multi-user MIMO-OFDM: complexity and performance," *EURASIP Journal on Wireless Communications and Networking*, vol. 2012, no. 1, p. 75, 2012.

[10] C.-H. Yih, "Effects of channel estimation error in the presence of CFO on OFDM BER in frequency-selective Rayleigh fading channels," *JCM*, vol. 3, no. 3, pp. 10–18, 2008.

[11] J. G. Proakis, *Digital Communications*. New York: McGraw-Hill, 2001.

[12] P. Hoeher, S. Kaiser, and P. Robertson, "Two-dimensional pilot-symbol-aided channel estimation by Wiener filtering," *IEEE International Conference on Acoustics, Speech, and Signal Processing (ICASSP'97)*, vol. 3, pp. 1845–1848 vol.3, 1997.

[13] G. Auer and E. Karipidis, "Pilot aided channel estimation for OFDM: a separated approach for smoothing and interpolation," in *2005 IEEE International Conference on Communications (ICC'2005)*, vol. 4, 2005, pp. 2173–2178 Vol. 4.

[14] P. Hoeher, "A statistical discrete-time model for the WSSUS multipath channel," *IEEE Transactions on Vehicular Technology*, vol. 41, no. 4, pp. 461–468, 1992.

[15] P. Hoeher, S. Kaiser, and P. Robertson, "Pilot-symbol-aided channel estimation in time and frequency," in *In Proc. IEEE Global Telecommunications Conference (GLOBECOM 97), Communication Theory Mini-Conference*, 1997, pp. 90–96.

[16] M. Unser, "Splines: a perfect fit for signal and image processing," *Signal Processing Magazine, IEEE*, vol. 16, no. 6, pp. 22–38, 1999.

ISBN 978-3-8007-3584-6